Can polygenic-informed EEG biomarkers predict differential antidepressant treatment response? An EEG stratification marker for rTMS and sertraline

Martijn Arns (martijn@brainclinics.com)
Utrecht University https://orcid.org/0000-0002-0610-7613

Hannah Meijs
Brainclinics Foundation

Bochao Lin
University Medical Center Utrecht

Guido van Wingen
Amsterdam Medical Center

Evian Gordon
Brain Resource Center

Damiaan Denys
Amsterdam Medical Center, Amsterdam University

Bieke De Wilde
Ziekenhuis Netwerk Antwerpen

Jan Van Hecke
Ziekenhuis Netwerk Antwerpen

Pieter Niemegeers
Ziekenhuis Netwerk Antwerpen

Kristel van Eijk
University Medical Center Utrecht, Utrecht University

Jurjen Luykx
University Medical Center Utrecht, Utrecht University

Article

Keywords: biomarker, predictive markers, depression

Posted Date: February 5th, 2021

DOI: https://doi.org/10.21203/rs.3.rs-155886/v1

Abstract

The treatment of major depressive disorder (MDD) is hampered by low chances of treatment response in each treatment step, which is partly due to a lack of firmly established outcome-predictive biomarkers. Here, we hypothesize that polygenic-informed EEG biomarkers may help predict differential antidepressant treatment response. Using a polygenic-informed electroencephalography (EEG) data-driven, data-reduction approach, we identify a functional brain network that is sex-specifically associated with polygenic risk for MDD in psychiatric patients (N=1,123). Subsequently, we demonstrate the utility of this network in predicting response to transcranial magnetic stimulation (TMS) and antidepressant medication in two independent datasets (N=196 and N=1,008). A simulation aimed at stratifying patients to TMS, sertraline or escitalopram/venlafaxine based on only this EEG component yields up to >30% improved remission rates. Overall, our findings highlight the power and utility of a combined polygenic and neurophysiological approach in the search for clinically-relevant biomarkers in psychiatric disorders.

Introduction

Major depressive disorder (MDD) is a common psychiatric disorder with a complex etiology that is generally explained from a biopsychosocial model, in which multiple biological, psychological, and social factors are all considered important contributors.[1,2] Furthermore, genetic risk factors of MDD overlap with other psychiatric disorders.[3] It is assumed that this multifactorial model for MDD underlies its heterogeneous symptomatology and variable treatment efficacy,[4,5] as well as the higher prevalence and different presentation of MDD in women compared to men.[6,7]

In line with the biological heterogeneity of MDD that in turn may be related to treatment outcome, pharmacogenomic studies have focused on genetic biomarkers of antidepressant treatment response in MDD. Genome wide association studies (GWASs) have identified several (common) genetic variants that are associated with antidepressant efficacy, but clinically-relevant and converging evidence has remained elusive.[8–15] For repetitive transcranial magnetic stimulation (rTMS) responsiveness, to our knowledge, only one GWAS at relatively limited power is available.[16] Thus, antidepressant treatment outcome is likely a complex trait and explained by several loci of small effect,[17] with recent evidence indeed suggesting that antidepressant response is polygenic.[18] Consequently, a polygenic instead of single gene or locus approach, by calculation of the individual's polygenic risk score (PRS) seems valuable to associate genetic risk with treatment (non)response.[19] However, despite recent evidence showing the power of PRS of MDD for a range of MDD-related phenotypes,[20] at present evidence for the out-of-sample value of polygenic risk approaches in the prediction of treatment outcome is limited.[18,21–24] A proposed strategy to effectively predict therapeutic outcomes for clinically prognostic purposes, is to integrate PRS with other predictors, such as neuroimaging and clinical characteristics.[25]

Electroencephalography (EEG) is a non-invasive neuroimaging technique that is used to quantitatively analyze oscillatory brain activity of neurons with high temporal resolution.[26] Several EEG patterns are

heritable, in particular characteristics within the alpha frequency band and EEG power across the power spectrum.[27–30] Some studies have also demonstrated heritability for functional connectivity and ('small world') network organization parameters, which have been linked to pathological states of the brain.[31–33]

EEG biomarker research for treatment prediction within MDD has shown that certain EEG patterns or abnormalities are differentially associated with *drug-specific* or *drug-class* specific antidepressant treatment effects[34–36], as well as rTMS outcome.[37–40] Such studies have also demonstrated qualitative sex differences in topographic distribution of EEG activity and sex-specific predictors of treatment response of alpha asymmetry,[35] EEG connectivity,[41] and event-related potentials.[42] Until recently, it was concluded that studies are insufficiently validated and replicated, and do not yet support the use of EEG for clinical decision making.[43] However, two recent studies using machine-learning algorithms applied to resting-state EEG features identified predictive signatures for sertraline, a selective serotonin-reuptake inhibitor, that related differentially to rTMS response.[44,45] This finding is of clinical relevance as it suggests that EEG signatures may be useful as a clinical tool to stratify patients to one of two evidence-based antidepressant treatments (rTMS vs. antidepressant medication), aiming to increase initial treatment response, without the requirement to consider off-label prescriptions or simply 'withhold' treatment due to a biomarker predicting low likelihood of response.[46]

Here, our aim was to predict treatment outcome in MDD based on an EEG biomarker using a polygenic-informed EEG data-driven, data-reduction approach: selection of functional brain networks for subsequent response prediction was guided by PRS-MDD, thus combining genetics with neurophysiology approaches. To that end, we conducted a functional independent component analysis (fICA) using LORETA (Low Resolution Brain Electromagnetic Tomography), producing independent spectral-spatial components (i.e. functional brain networks), in a large dataset of severely ill psychiatric patients and healthy controls (dataset 1). In a prior study, this fICA method was tested and validated,[47,48] and demonstrated to reliably identify the default mode network (DMN) and task-positive network (TP) in a sample of 1,397 subjects, replicated in an independent ADHD sample.[47] We then found that one functional network was significantly associated with polygenic liability to MDD. Subsequently, validation analyses in two large independent datasets (datasets 2 and 3) demonstrated how this EEG biomarker is differentially associated with antidepressant treatment to rTMS and antidepressant medication. Finally, in simulation approaches we show that this biomarker increases prediction accuracy of antidepressant treatment response and remission, by stratification to one of two treatments by the EEG biomarker.

Results

An overview of the baseline demographic characteristics and response and remission rates per dataset after EEG preprocessing (online Methods) can be found in Table 1. The analysis procedure that was performed in this study is visualized in Figure 1.

ICA analysis identifies 58 components

Of the 1,195 participants enrolled in dataset 1, the final sample for the LORETA-fICA analysis after quality control (online Methods) consisted of 1,061 hospital-admitted psychiatric patients and 62 healthy controls (N=1,123; dataset 1). The appropriate dimensionality of the data was established using sphericity test which indicated 58.2 dimensions; hence the LORETA-fICA analysis was constrained to 58 components that explained 96.0% of the total variance in EEG power (see Figure 1: discovery).

Relating components to polygenic risk for MDD

Of the 1,123 participants, PRS-MDD association analysis was performed using the data of 722 participants remaining after EEG pre-processing and genetic quality control (Supplementary information). The individual loading score on 1 out of 58 independent components correlated negatively (r=-0.182, R^2=3.3%) at p<0.001 with PRS-MDD at $P_T<5.0\times10^{-8}$, after controlling for age and the first five genetic principal components (PCs), in women only (see Supplementary information for more details about the PRS model fit). This was followed up by an exploratory SNP analysis separately for men and women, which revealed that – for five variants – the component loading was significantly different between homozygotes or heterozygotes for the alternate allele compared to homozygotes for the reference allele (see Supplementary information for all results). Notably, the loading was significantly different in subjects with a homozygote variant on the *SGIP1* (SH3 domain GRB2 like endophilin interacting protein 1) gene (rs6656912) compared to those homozygotes for the reference allele, which was more pronounced and in opposite direction in men (Cohen's d, d=-0.435; p=0.007) compared to women (d=0.310; p=0.041).

Figure 2 shows the component that was associated with PRS-MDD in women, representing jointly deactivation and activation of neural activities coming from sets of regions that form functional spatial-spectral networks (see Supplementary information for a non-scaled color map of the networks). Most prominent were frontal alpha power, mainly seen at the left dorsolateral prefrontal cortex (DLPFC), inversely associated with delta and theta power in the right anterior portion of the PFC and delta power seen at a region surrounding the left lateral sulcus, mainly including somatosensory-motor cortices. We will refer to this component as the prefrontal and sensorimotor (PF-SM) network.

The individual loadings on the PF-SM network as visualized in Figure 2, did not correlate with baseline characteristics and a sensitivity analysis revealed that the displayed results cannot be explained by frontal alpha asymmetry, as earlier reported by Arns et al.[35] on the same data (see Supplementary information for the correlation sensitivity analysis), thus ruling out that only the asymmetric alpha was predictive and therefore this represents a novel EEG biomarker.

Relating the PRS-informed EEG component to antidepressant treatment outcomes

The primary outcome for validation analysis (see Figure 1: validation) was dimensional improvement of depressive symptoms using linear regression, based on self-report questionnaire scores at baseline and after rTMS (dataset 2) or medication treatment (dataset 3). All data were normally distributed. The secondary analysis was focused on categorical improvement: response (defined as ≥50% reduction of

baseline severity score) and remission (defined as a score of ≤12 on the Beck Depression Inventory II, BDI-II, or ≤5 on the Quick Inventory of Depressive Symptomatology, QIDS).

Relating the PRS-informed EEG component to rTMS outcome (dataset 2)

Of the 196 participants, data of 186 were usable (receiving rTMS 1 Hz right DLPFC or 10 Hz left DLPFC, clean EEG and all channels available).

Primary linear regression analysis of ΔBDI-II on individual EEG component loading with age as covariate yielded an R^2 of 7.9% (p=0.007) in women, and R^2 of 8.0% (p=0.005) in men, and R^2 of respectively 6.7% (p=0.009) and 6.4% (p=0.008) when baseline BDI-II score was also added as covariate.

Second, ANCOVA with EEG component loading as dependent variable and response and sex as fixed factors, and age as covariate yielded a significant response x sex interaction (F(1,181)=6.871; p=0.010). Repeating the analysis for men and women separately resulted in a main effect of response for men (*d*=0.596; F(1,90)=9.747; p=0.002), and no main effect for women. A discriminant analysis showed that age significantly predicted response in men (Wilk's Lambda=0.936; Chi-Square=5.945; p=0.015), and including EEG component loading to the model resulted in an improved prediction model (Wilk's Lambda=0.845; Chi-Square=15.167; p=0.001). The PPV and NPV were 0.81 and 0.59, respectively. The ROC for this model yielded an area under the curve (AUC) of 0.735 (see Figure 3A).

ANCOVA with EEG component loading as dependent variable and remission and sex as fixed factors, and age and baseline BDI-II score as covariates yielded a significant remission x sex interaction (F(1,180)=9.304; p=0.003). Repeating the analysis for men and women separately resulted in a main effect of remission for women (*d*=-0.439; F(1,89)=7.792; p=0.006) and men (*d*=0.438; F(1,89)=7.304; p=0.008), but in opposite direction. A discriminant analysis revealed that age and baseline BDI-II significantly predicted remission in both women (Wilk's Lambda=0.737; Chi-Square=27.481; p<0.0001) and men (Wilk's Lambda=0.875; Chi-Square=11.984; p=0.002). Again, prediction improved when EEG component loading was added to the model in women (Wilk's Lambda=0.678; Chi-Square=34.840; p<0.0001) and men (Wilk's Lambda=0.809; Chi-Square=18.977; p=0.0003). This model resulted in a PPV of 0.77 and NPV of 0.73 in women, and PPV of 0.69 and NPV of 0.58 in men. The ROC for this analysis yielded an AUC of 0.815 in women and AUC of 0.744 in men (see Figure 3B).

A sensitivity analysis confirmed that EEG component loading alone significantly contributed to the rTMS response and remission prediction models as outlined above (see Supplementary information for discriminant sensitivity analysis).

To explore if findings were driven by one of the two rTMS protocols (1 Hz R-DLPFC vs. 10 Hz L-DLPFC rTMS) a sensitivity analysis was performed. For response, running the ANCOVAs as above, adding rTMS protocol as fixed factor, yielded a significant main effect for 10 Hz rTMS in men only (*d*=0.963; F(1,34)=9.752; p=0.004), but not for 1 Hz rTMS, albeit the effect was in the same direction (*d*=0.295). This indicates the effect on response in men was mostly attributable to 10 Hz rTMS. For remission, no

significant interactions with rTMS protocol were found (see Supplementary information for detailed outline of the interactions and results).

Relating the PRS-informed EEG component to antidepressant medication outcome (dataset 3)

Of the 1,008 participants, data of 535 were usable (treated per protocol, clean EEG and all channels available).

Primary linear regression analysis of ΔQIDS on individual EEG component loading with age as covariate yielded an R^2 of 3.1% (p=0.015) in all subjects (men and women together) receiving sertraline treatment, and R^2 of 2.4% (p=0.019) when baseline QIDS score was also added as covariate. No significant associations were found within subjects receiving escitalopram or venlafaxine.

Second, ANCOVA with EEG component loading as dependent variable and response and sex as fixed factors, and age as covariate yielded a significant response x treatment interaction (F(2,489)=3.278; p=0.039), but no interaction with sex. Repeating the analysis for all three antidepressants separately without treatment as fixed factor resulted in a main effect of response for sertraline (*d*=-0.309; F(1,177)=4.316; p=0.039). A discriminant analysis resulted in a significant contribution of age to the prediction of sertraline response in women and men together (Wilk's Lambda=0.970; Chi-Square=5.431; p=0.020). Running the same analysis including the EEG component loading resulted in an improved model (Wilk's Lambda=0.948; Chi-Square=9.618; p=0.008), with a PPV and NPV of 0.60 and 0.55, respectively. The AUC of the ROC analysis was 0.634 (see Figure 3A).

ANCOVA with EEG component loading as dependent variable and remission and sex as fixed factors, and age and baseline QIDS score as covariates yielded no significant interactions, suggesting the increased network activity is predictive for sertraline response, but not remission when controlled for baseline symptom severity.

A sensitivity analysis confirmed that EEG component loading alone significantly contributed to the sertraline prediction model for response as outlined above (see Supplementary information for discriminant sensitivity analysis).

Stratification demonstrates likelihood of remission is increased when using the EEG component

Based on the merged (significant) changes of self-report scores against the PF-SM network loading (Figure 4A), a simulation was conducted to assess the improvement in treatment outcome, using a cut-off of zero (Figure 4B). To that end, we calculated what the effect would have been (see Figure 4C) if women with greater (>0) and men with lower (<0) loadings than zero had been treated with rTMS, and if men or women with greater loading (>0) than zero had been prescribed sertraline (see Supplementary information for details of this simulation). The remission rate to rTMS (10 Hz L-DLPFC or 1 Hz R-DLPFC) would have improved from 55% to 69% in women (+26%) and from 56% to 62% in men (+11%). The improvement was largest for 10 Hz rTMS: from 58% to 75% in women (+29%) and from 59% to 70% in

men (+18%). The remission rate to sertraline would have improved from 35% to 46% in men and women (+34%). The rTMS response rate in men would have improved from 61% to 68% in men (+11%), and was largest for 10 Hz rTMS, in line with our rTMS protocol sensitivity analysis outlined above: from 68% to 80% (+18%). The response rate to sertraline would have improved from 53% to 69% (+30%). Women with a loading smaller than zero would respond less to both sertraline and rTMS and treatment with escitalopram or venlafaxine would result in slightly improved remission and response rates for them (+5% and +4%, respectively).

Discussion

Here, we aimed to elucidate whether polygenic-informed EEG biomarkers may help predict differential antidepressant treatment response. Using a polygenic risk score-informed data-driven, data-reduction approach applied to resting-state EEG in a large set of hospital-admitted psychiatric patients and healthy controls (dataset 1), we were able to identify one spectral-spatial independent component ('functional network'). Given psychological measures mapping poorly on neurobiology and cognizant of the scarce diagnostic and prognostic biomarkers in MDD,[49–51] we have here taken a novel, genetics-informed approach. We thus uncovered a functional network biomarker that in turn was differentially associated with two evidence-based antidepressant treatments in independent datasets.

Visualizing our functional network (Figure 2), we found 1) prefrontal jointly left-sided alpha power (mainly DLPFC) that was inversely associated with right-sided slow delta and theta power (mainly in the anterior portion of the PFC); 2) slow delta power surrounding the left lateral sulcus, including the somatosensory-motor and auditory cortex; 3) asymmetrical alpha activity in the visual cortex. The individual strength of this PF-SM network was differentially associated with treatment outcomes to rTMS in a sex-specific manner, and to sertraline (similar for men and women), but no such associations for escitalopram or venlafaxine were detected.

In women, but not in men, increased neural activity of this network was related to lower PRS-MDD. The predictive value of the network with regards to treatment outcome was validated in MDD patients receiving TMS treatment (dataset 2) and randomized antidepressant treatment (dataset 3). Primary analysis showed that increased network PF-SM strength was dimensionally associated with response to rTMS in women but to non-response in men, while it was non-sex-specifically associated with sertraline response. Secondary analysis confirmed these results for remission from MDD. Subsequent discriminant analysis suggested that the PF-SM network loading improved the basic model including the clinical variables age and baseline severity symptom score for the prediction of remission and response. Lastly, based on the relative change on self-reporting questionnaires, a clinical cut-off individual PF-SM network loading of 0 was established. The results of the simulation indicated an improvement in the number of predicted rTMS remitters with 11%-26% and of sertraline remitters with 34%. Rest-EEG recordings and subsequent calculation of PF-SM network loading in treatment-naive MDD patients before treatment inception is likely relatively economical and non-invasive. Such a simulation may thus in future provide a useful construct for treatment stratification, thereby enhancing chances of initial remission (and

response), thus limiting the relative inefficiency of the current stepped-care, 'trial-and-error' approach. For example, if the loading value for a given patient is >0, a clinician may decide to prescribe sertraline and alternatively advise rTMS for female MDD patients. If the loading value is <0, they may choose rTMS for a male patient, but escitalopram or venlafaxine for a female patient. Given that efficacy of antidepressant treatment in the general MDD population is moderate,[52–54] and antidepressant discontinuation and switching rates are high,[55–57] only slightly increased response chances may reduce disease burden and duration.

Several hypotheses might explain the predictive value of the PF-SM network for antidepressant treatment outcomes in MDD. Abnormalities of the PFC as a network node are known to be implicated in the etiology of MDD and have previously been associated with treatment outcome.[58] TMS applied to the PFC, however, results in transsynaptic activation of deeper areas such as the sgACC,[59] and the frontal-vagal pathway.[60] It is plausible that, by modulating neural activity at the stimulation site, TMS synchronically activates remote cortical areas and thereby modulates dysfunctional functional connectivity between areas of the PF-SM network in a cross-frequency manner. An organized neural circuit between the PFC and motor and somatosensory cortices has been described.[61] Also, TMS induces anticorrelations between the DLPFC and medial prefrontal areas of the default mode network.[62] Notably, the effect we detected was mostly driven by high frequency (10 Hz) stimulation at the left DLPFC, which was previously associated with a network synchronizing effect in the alpha frequency band.[40] This protocol-specific effect was most predominantly found in men. Furthermore, while increasing PF-SM network activity was significantly related to improvement of depressive symptoms after rTMS in women, the reverse effect was found in men. These findings hint at different underlying mechanisms of action of TMS on neural activity in men relative to women, and are supported by previous studies reporting sex-specific differences in TMS response.[63–65] On a SNP level, the PF-SM network loading was also different in subjects homozygous for the rs6656912 variant (*SGIP1*), compared to reference allele homozygotes, which was more pronounced and in opposite direction in men compared to women. *SGIP1* is expressed predominantly in the brain and encodes a protein required for the neuronal regulation of energy homeostasis.[66] Recently, it was hypothesized that *SGIP1* may be involved in processes regulated by Wnt signaling, together with other protein interactors of Wntless (Wl, essential protein for the secretion of multiple Wnt proteins[67]) that are expressed in the brain, such as the dopamine transporter.[68] Differences in Wnt signaling may partly underlie the reversed treatment outcomes found men and women. Further research is warranted to investigate these sex-specific mechanisms.

In both sexes, increased PF-SM network activity was antidepressant-specifically related to sertraline response, but not to escitalopram or venlafaxine. Sertraline, in contrast to the other two antidepressants, is also a synaptic dopamine reuptake inhibitor that increases extracellular levels of dopamine.[69,70] Potential involvement of dopamine in the PF-SM network is supported by the finding that rTMS of the left PFC can induce dopamine release in the striatum.[71] Dopamine plays a prominent role in many functions that are impaired in MDD, such as execution of movement, executive cognitive functioning, and the ability

to experience pleasure.[72] Downregulation of the dopamine system, leading to dysfunction of neural circuits such as PFC-amygdala functional connectivity, has been implicated in the pathophysiology of MDD.[73] Evidence also suggests involvement of dopaminergic systems in the modulation of sensorimotor gating,[74] and indicates that MDD is characterized by dysregulation of sensorimotor processes that modulate depressive symptoms via fronto-limbic circuits.[75,76] Thus, the PF-SM network we uncover here may partly reflect a disrupted dopamine system, and therefore allows sertraline outcome prediction.

Cross-validation using three large, independent datasets is an important strength of this study. In addition, the fICA-LORETA method is applicable to all EEGs independently of apparatus, electrode configuration or number of electrodes since it is derived from the voxel-level rather than the electrode level. Furthermore, to allow for future clinical translation of our findings we have highlighted several clinically intuitive outcome measures that indicate clinical relevance of the EEG component we retrieve. Nonetheless, limitations of our study include the lack of a placebo control arm, precluding analyses that parse placebo effects. On the other hand, the opposite effects for men and women for rTMS argue against notion of none-specific effects. Since all patients received psychotherapy concurrent with rTMS, we could not rule out that the EEG component was predictive for rTMS only. Furthermore, for visualization of neural activity, the fICA-LORETA method calculates power on a categorical scale (i.e. frequency bands) instead of a continuous scale (i.e. power spectrum), thereby limiting the interpretation of the functional networks that are obtained by fICA. Finally, while for our stratification model we relied on an EEG biomarker, future studies should aim to further optimize stratification by also including other baseline variables, which are likely to further improve the clinical response.

In conclusion, we show for the first time how a genetics-informed data-driven, data-reduction approach identifies an EEG functional brain network that increases response prediction to two treatments in MDD. Our method highlights the clinical applicability of such an approach and sets the stage for future stratified psychiatry research.

Online Methods

Participants, dataset 1

The first dataset was used for functional independent component analysis (fICA). EEG recordings of participants potentially eligible were collected from September 2013 until September 2018 at Ziekenhuis Netwerk Antwerpen (ZNA), a large community hospital in Antwerp, Belgium. The study was approved by the Institutional Review Board of ZNA. We abided by the principles of the Declaration of Helsinki. A total of 1,195 adult participants – 1,132 psychiatric patients and 63 healthy controls – were included and provided written informed consent. Exclusion criteria for all participants were age < 18 years, inability to give informed consent for whatever reason, restlessness that could interfere with the EEG, and inability to sit still. Only patients who were hospital-admitted for stabilization and/or treatment of a psychiatric disease (no further selection was made) were included to allow collection of a representative and heterogenous cohort of (severely ill) psychiatric patients. Healthy controls were defined as having no

current psychiatric episode and never been treated by a mental health service. After preprocessing, the total sample for fICA consisted of 1,123 (1,061 patients and 62 healthy controls).

Participants of the rTMS study, dataset 2

The second dataset was used for validation purposes and the evaluation of treatment effects. It consisted of 196 patients, diagnosed with non-psychotic MDD or dysthymia and BDI-II ≥14 at baseline, receiving protocolized rTMS treatment concurrent with psychotherapy. All participants provided written informed consent. Only participants receiving high-frequency TMS (10 Hz left dorsolateral prefrontal cortex, DLPFC) or low-frequency TMS (1 Hz right DLPFC) were included; participants receiving both 1 Hz and 10 Hz sequentially were excluded since this would make interpretation of results difficult. All patients completed at least 10 sessions of treatment, and filled in the BDI-II at baseline and at the last session (on average session 21). Details about this sample are described elsewhere.[49,77]

Participants of the medication study, dataset 3

The third dataset used for validation purposes and the evaluation of treatment effects was an international multi-center, randomized, prospective open-label trial (phase-IV clinical trial), or iSPOT-D sample (International Study to Predict Optimized Treatment in Depression). This study consisted of 1,008 patients diagnosed with non-psychotic MDD who were subsequently randomized to escitalopram, sertraline, or venlafaxine. All participants provided written informed consent and this study was approved by the institutional review boards at all of the participating sites and this trial was registered with ClinicalTrials.gov under id NCT00693849. At baseline and after 8 weeks of treatment patients filled in the Quick Inventory of Depressive Symptomatology (QIDS). Only data from participants who completed 8 weeks of randomized medication treatment ('per protocol' sample) were included. Details about this sample have been published elsewhere.[35,78]

DNA isolation and genotyping (dataset 1)

DNA was isolated and genotyped for 887 participants who provided informed consent for DNA extraction and analyses. One 10 ml ethylenediaminetetraacetic acid (EDTA) tube was filled during standard blood draws at the ward. DNA was extracted in the clinical molecular genetics laboratory of the University Medical Center Utrecht (UMCU). Samples were brought to a DNA concentration of 50 ng/µl with a total concentration of 200 ng DNA per participant. Subsequently, samples were sent in two batches to the Human Genotyping Facility of Erasmus Medical Center (Erasmus MC) Rotterdam for Global Screening Array v.1 (GSA) by Illumina, Santa Clara (California), USA, that has excellent validity and reliability.[79]

Genetic quality control (dataset 1)

Quality control (QC) and principal component analysis (PCA) were done with PLINK 1.9,[80] and performed on two batches separately (see Supplementary information). Pre-imputation involved the creation of a superset with the highest quality SNPs for subsequent sample QC. The superset of SNPs was created by

excluding those with genotype call rates <0.01, minor allele frequencies (MAF) <0.1, Hardy-Weinberg equilibrium (HWE) $<10^{-4}$, and linkage disequilibrium (LD) r^2 >0.2, with a window size of 50 and window shifting of a step size of 5. Using the superset, subjects were removed who: 1) had a mismatch in their sex between reported and genotyped; 2) were too extremely hetero- or homozygous (their F-values differed ≥3 SDs from the mean in the whole cohort); 3) were related (their pi-hat was above 0.1: one of each pair was randomly excluded); and 4) were cohort outliers (had values for the first two ancestry principal components (PCs) that deviated ≥3 SDs from the mean of the whole cohort).

This was followed by a regular SNP-level QC for exclusion of ill performing SNPs: variants with genotyping rate <0.01; MAF < 0.01; HWE p-value $<10^{-5}$ were thus excluded. European ancestry was checked by comparing with the HapMap population: individuals were removed who deviated ≥3 SDs from the first and second genetic ancestry PCs from the Northern and Western European (CEU) population.

Lastly, before imputation, genotypic data was compared with the Haplotype Reference Consortium panel. Strands, alleles, positions and frequency differences were checked. Chromosomes were pre-phased and imputed using the Michigan Imputation Server.[81] Post-imputation QC was performed to include reliable SNPs: variants that had a MAF >0.05 and LD r^2 ≥0.8 were included, resulting in 5,211,700 SNPs available to generate PRS.

Polygenic risk score calculation (dataset 1)

The polygenic risk score (PRS) for MDD per individual was generated for those SNPs and individuals remaining after QC. The summary statistics of MDD (meta-analysis of PGC and UK Biobank[82]) were used to generate PRSs.[83] That dataset has no sample overlap with the current dataset as Belgian individuals had not been included in the large MDD GWAS. If only odds ratios (ORs) were reported in the summary statistics, ORs were log-converted to beta values as effect sizes. To that end, the beta values, effective allele, and p-values were extracted from all summary statistics.

SNPs that overlapped between the summary statistics GWASs (training datasets), 1,000 genomes (reference), and our dataset (target) were extracted. Then, insertions or deletions, and ambiguous SNPs, were excluded. To account for complicated LD structure of SNPs in the genome, these SNPs were clumped in two rounds using PLINK 1.90b3z,[84] according to previously established methods;[85,86] round 1 with the default parameters (physical distance threshold 250 kb and LD threshold (r^2) 0.5); round 2 with a physical distance threshold of 5,000 kb and LD threshold (r^2) 0.2. Additionally, we excluded all SNPs in genomic regions with strong or complex LD structures. Sample overlap between training datasets with our target samples is unlikely since all samples belong to different cohorts and to our knowledge no Belgians had been included in the aforementioned GWASs.

We constructed PRSs based on risk alleles weighted by their effect sizes estimate using PLINK's score function for 12 GWAS p-value thresholds (P_T)[81,87]: 5×10^{-8}, 5×10^{-7}, 5×10^{-6}, 5×10^{-5}, 5×10^{-4}, 5×10^{-3}, 0.05, 0.1,

0.2, 0.3, 0.4, 0.5 and 1.

EEG recordings and preprocessing

During EEG recordings, subjects were seated in a sound and light attenuated room that was controlled at an ambient temperature of around 22°C. The participants were instructed to sit still for the duration of the recording without thought instructions. The operator did not intervene when drowsiness patterns were observed in the EEG.

Resting-state eyes closed EEG recordings for dataset 1 were acquired from 65 channels of the Electrical Geodesics Incorporated (EGI; Magstim, UK) system (dataset 1) and from 26 channels (10-20 electrode international system: Fp1, Fp2, F7, F3, Fz, F4, F8, FC3, FCz, FC4, T3, C3, Cz, C4, T4, CP3, CPz, CP4, T5, P3, Pz, P4, T6, O1, Oz, and O2) of the Neuroscan NuAmps (Compumedics, Australia; dataset 2 and 3). Data were recorded for three (dataset 1) or two (dataset 2 and 3) minutes during eyes closed condition. The sampling frequency was 500 Hz for most recordings, but 1,000 Hz for 6 recordings in dataset 1 (which were down-sampled to 500 Hz prior to further analyses). Data were referenced to Cz (dataset 1) or average mastoids with a ground at AFz (dataset 2 and 3). Horizontal eye movements were recorded with electrodes 61 and 64 (dataset 1) or electrodes placed 1.5 cm lateral to the outer canthus of each eye (dataset 2 and 3). Vertical eye movements were recorded with electrodes 5 and 62 (dataset 1) or electrodes placed 3 mm above the middle of the left eyebrow and 1.5 cm below the middle of the left bottom eyelid (dataset 2 and 3). Cartesian coordinates of the EGI system electrodes (dataset 1) were converted to spherical coordinates prior to EEG preprocessing.

Subsequently, the following steps were taken in the EEG preprocessing and artefact rejection procedure using Brain Vision Analyzer 2.0 (Brain Products, Germany): 1) data filtering: 0.5-90 Hz (dataset 1) or 0.3-100 Hz (dataset 2 and 3), and notch filter; 2) removal and spherical spline interpolation of noisy signals or flat lines; 3) electro-oculography (EOG) correction, using a regression-based technique[88]; 4) segmentation in 4-second epochs; and 4) artefact-rejection using an automatic procedure (criteria: maximal allowed difference of 150 μV peak-to-peak). This resulted in a minimum of one-minute data per subject.

LORETA-fICA model

The EEG was used for estimating the cortical source distribution of electric neuronal activity by means of LORETA (low-resolution electromagnetic tomography; free academic software available at https://www.uzh.ch/keyinst/loreta). This method weights minimum norm inverse solution, and localization inference is based on the standardized estimates of the current density.[89]

The following analysis steps were performed using the collection of 4-second artefact-free epochs obtained from dataset 1. In the first step, each EEG recording was transformed to the frequency domain, using the discrete Fourier transform. The cross-spectral matrices were obtained for six frequency bands, defined as: delta (1.5-3.5 Hz), theta (4-7.5 Hz), alpha (8-13 Hz), beta (14.5-30 Hz), low-gamma (31-47 Hz),

and high-gamma (>70 Hz). Aiming to eliminate the notch bands used at different sites in the EU and US, the 48-69 Hz range was excluded. In the second step, from data of each cross-spectrum matrix, the spectral density was computed for each cortical voxel, sampled at 5 mm resolution in a realistic head model, using the MNI152 template.[48] In the third step, the spectral-spatial data of all subjects was concatenated, and ICA was performed on this data, aiming to identifying independent spectral-spatial components (i.e. functional networks). This method was recently validated in Aoki et al. and Gerrits et al. and reliable identified DMN (default mode network) and TP (task-positive) networks.[47,48]

The typical ICA model assumes that the source signals are not observable, statistically independent and non-Gaussian, with an unknown, but linear, mixing process,[90] and is described by the following formula:

$x=As$

where x, A and s represent matrices. In our case, these three matrices consisted of the following data:

1. Matrix x with 1,123 rows corresponding to all subjects of dataset 1, and the data per subject consists of 37,434 (6,239x6) columns corresponding to the spectral power at 6,239 cortical voxels for the six frequency bands. This approach, using a priori determined frequency bands, is a unique feature of the method used.[91]
2. Matrix s with 58 rows corresponding to the number of statistically independent components (i.e. functional networks), and 37,434 columns. In this way, each functional network contains 6 spatial images corresponding to the neural activity of each frequency band (i.e. in a cross-frequency manner).
3. Matrix A with 1,123 rows and 58 columns. Thus, what remains of this data reduction for every subject is the amount of each component that was used for that subject. This amount is expressed as a loading (i.e. signed weight or score) per functional network for each subject.

Independent components

Each independent cross-frequency spectral-spatial functional network (fICA network or EEG component) represents sets of brain regions that are consistently activated or deactivated together within and across a given frequency band. The number of EEG components here was estimated from a measure related to Wackermann's Omega Complexity,[92] indicating 58.2 dimensions, hence the LORETA-fICA analysis was constrained to 58 components explaining 96.0% of total EEG power variance, which is a great reduction of data.

To visualize the functional networks (i.e. correlation of brain regions that are consistently activated or deactivated), a threshold at 3 z-values was set. Individual loadings per fICA network were obtained for each subject, corresponding to the strength of that network for a given individual subject.

The functional networks that were established based on the first dataset, were prospectively applied to dataset 2 and 3. Likewise, for each subject in each dataset, EEG component loadings were obtained per

network. These loadings were used in the statistical analysis.

Outcome measures

For biomarker identification (discovery, Figure 1 main text) PRS-MDD was examined for association with independent EEG components (dataset 1). The primary outcome for the prediction analysis (validation, Figure 1 main text) was dimensional improvement of depressive symptoms, based on the BDI-II for rTMS sample (dataset 2) and the QIDS for iSPOT-D sample (dataset 3), which are both self-report questionnaires. In a secondary analysis we focused on categorical improvement defined as response or remission. Self-reports were taken at intake and after treatment completion (on average at session 21 for rTMS and at week 8 for antidepressants). Response was defined as ≥50% reduction of baseline score, while remission was defined as a score of ≤12 on the BDI-II[93] (dataset 2) or ≤5 on the QIDS[94] (dataset 3).

Statistics

SPSS version 26 was used for statistical analyses. Effects sizes (ES) of significant main effects are reported as R^2 for continuous measures or as Cohen's d (*d*) for binary measures. Two-sided tests were performed for statistical significance testing.

A priori, analyses were stratified by sex, since previous iSPOT-D studies reported sex-specific predictors of treatment outcome,[35,41,42,78] and this would enable us to identify stratification biomarkers. Hence, sex was included as main factor or women and men were analyzed separately if the analysis could not accommodate sex as main factor, rather than handled as covariate since covariation can only resolve quantitative – not qualitative – sex differences. If no sex interaction was found or the effect for both sexes was the same direction, men and women were analyzed together.

First, a discovery analysis was performed to examine if there was an association between one or more fICA components and PRS-MDD (dataset 1). To that end, a partial correlation analysis – controlling for age and the first five genetic ancestry principal components (PCs) on men and women separately – was run between all EEG fICA components loadings and the most stringent PRS-MDD p-value thresholds ($P_T=5.0\times10^{-8}$ to $P_T=0.05$) in order to choose the optimal P_T, which is unknown a priori.[83] The significance level was set to $\alpha<0.001$, to obtain a highly significant result and reduce the likelihood of false positives and non-reproducibility of findings.[95]

Second, validation analyses were performed (dataset 2 and 3) to examine if the EEG component that was found to be significantly associated with the PRS-MDD in the discovery analysis, was predictive of treatment outcome (dataset 2 and 3). The significance cut-off for the analyses following up was set at conventional $\alpha=0.05$ as these analyses were intended for validation of the findings in the discovery analysis. We investigated possible associations between individual EEG component loading and absolute changes in BDI-II score (dataset 2) and QIDS score (dataset 3). The absolute change (Δ) was defined as the symptom severity score difference between baseline and at treatment completion. Therefore, for men

and women separately, ΔBDI-II and ΔQIDS were regressed on EEG component loading, adding age and baseline self-report score as covariates. If significant associations were found, factorial ANCOVAs were run to investigate if the individual loadings on the EEG component were significantly different in remitting and responsive patients relative to non-remitters and non-responders, respectively. In dataset 2, treatment response/remission and sex were added as fixed factors; in dataset 3, treatment response/remission, sex and antidepressant subtype were added as fixed factors. Age was added as covariate in all models. For remission, baseline BDI-II in dataset 2 and QIDS in dataset 3 (i.e. clinical score) were added as additional covariate, since baseline severity was related to treatment remission, while response was not.[49,78]

Subsequently, to assess the predictive value of the EEG component, a discriminant analysis on treatment outcome was performed for datasets 2 and 3. Prior studies had already tested several psychological (personality, anxiety etc.), demographic and behavioral measures and their ability to predict response or remission in these samples, and failed to find robust and clinically relevant predictors.[49,51] The baseline model consisted of 1) age predicting response and 2) age and baseline severity predicting remission. Then we tested whether the model performance improved when EEG component loading was added as a predictor. Also, a receiver operating curve (ROC) of both models was regressed on response and remission to establish the predictive value of the discriminant analysis. The positive predictive value (PPV) and negative predictive value (NPV) for predicting response and remission were assessed.

Finally, we attempted to make a construct, based on the data of both dataset 2 and dataset 3. In order to merge both samples, Z-scores of the ΔBDI-II and ΔQIDS were calculated. A clinical cut-off loading was visually determined based on a graph with dataset 2 and 3 merged, representing standardized ΔBDI-II and ΔQIDS against the EEG component loading. Based on this cut-off, a simulation was built in order to evaluate the clinical usefulness, by calculating the percentage response/remission improvement if only subjects above or below this cut-off were assigned to rTMS or sertraline treatment.

Declarations

Acknowledgements

We acknowledge the iSPOT-D Investigators Group, the contributions of iSPOT-D principal investigators at each site and the central management team (global coordinator Claire Day); Donna Palmer and Chris Spooner for support in the iSPOT-D data-analyses, Noralie Krepel, Vera Kruiver, Rosalinde van Ruth, Marleen Stam, Myrthe van Eerdt, Dagmar Timmers and for support and collecting the data used in the rTMS study and we thank Edwin van Dellen for advising on and critical appraisal of the methods and results.

Author Contributions

All authors have made substantial contributions to this study. JJL, BdW, JvH, PN, EG and MA collected data. HM, BL, KvE and MA processed and analyzed the data. HM and MA conducted the statistical analyses. HM, MA, JJL, GvW and DD interpreted the data. JJL and MA supervised the project. HM wrote

the first draft. All authors were involved in the writing and revision of further drafts, have approved the submitted version and agreed to be personally accountable for their own contributions.

Competing Interests statement

MA is unpaid chairman of the Brainclinics Foundation, a minority shareholder in neuroCare Group (Munich, Germany), and a co-inventor on 4 patent applications related to EEG, neuromodulation and psychophysiology, but receives no royalties related to these patents; Research Institute Brainclinics received research funding from Brain Resource (Sydney, Australia), Urgotech (France) and neuroCare Group (Munich, Germany), and equipment support from Deymed, neuroConn and Magventure. EG is founder and receives income as CEO and chairman for Brain Resource Ltd. and he has stock options in Brain Resource Ltd. Additional funding for this project was obtained through a personal UMC Utrecht Brain Center Rudolf Magnus Young Talent Fellowship (H150) to JL. The remaining authors, HM, BL, GvW, DD, BdW, JvH, PN and, KvE, declare no competing financial or non-financial interest.

Data Availability statement

The data that support the findings of this study are available from the corresponding author, MA, upon reasonable request.

References

1. Schotte, C. K. W., Bossche, B. V. D., Doncker, D. D., Claes, S. & Cosyns, P. A biopsychosocial model as a guide for psychoeducation and treatment of depression. *Depress Anxiety* **23**, 312–324 (2006).
2. Hasler, G. Pathophysiology of depression: do we have any solid evidence of interest to clinicians? *World Psychiatry* **9**, 155–161 (2010).
3. Smoller, J. W. *et al.* Identification of risk loci with shared effects on five major psychiatric disorders: a genome-wide analysis. *Lancet* **381**, 1371–1379 (2013).
4. Belmaker, R. H. & Agam, G. Major Depressive Disorder. *N Eng J Med* **358**, 55–68 (2008).
5. Rush, A. J. The Varied Clinical Presentations of Major Depressive Disorder. *J Clin Psychiatry* **68**, 4–10 (2007).
6. Gorman, J. M. Gender Differences in Depression and Response to Psychotropic Medication. *Gender Med* **3**, 93–109 (2006).
7. Kessler, R. C. Epidemiology of women and depression. *J Affect Disord* **74**, 5–13 (2003).
8. Ising, M. *et al.* A genome-wide association study points to multiple loci predicting antidepressant treatment outcome in depression. *Arch Gen Psychiatry* **66**, 966–975 (2009).
9. Garriock, H. A. *et al.* A Genome-Wide Association Study of Citalopram Response in Major Depressive Disorder. *Biol Psychiatry* **67**, 133–138 (2010).
10. Li, Q. S., Tian, C., Hinds, D. & Team, 23andMe Research. Genome-wide association studies of antidepressant class response and treatment-resistant depression. *Transl Psychiatry* **10**, 360 (2020).

11. Uher, R. *et al.* Genome-Wide Pharmacogenetics of Antidepressant Response in the GENDEP Project. *Am J Psychiatry* **167**, 555–564 (2010).
12. Fabbri, C. *et al.* New insights into the pharmacogenomics of antidepressant response from the GENDEP and STAR*D studies: rare variant analysis and high-density imputation. *Pharmacogenomics J* **18**, 413–421 (2018).
13. Ji, Y. *et al.* Pharmacogenomics of selective serotonin reuptake inhibitor treatment for major depressive disorder: genome-wide associations and functional genomics. *Pharmacogenomics J* **13**, 456–463 (2013).
14. Li, Q. S., Tian, C., Seabrook, G. R., Drevets, W. C. & Narayan, V. A. Analysis of 23andMe antidepressant efficacy survey data: implication of circadian rhythm and neuroplasticity in bupropion response. *Transl Psychiat* **6**, e889–e889 (2016).
15. Tansey, K. E. *et al.* Genetic Predictors of Response to Serotonergic and Noradrenergic Antidepressants in Major Depressive Disorder: A Genome-Wide Analysis of Individual-Level Data and a Meta-Analysis. *PLoS Med* **9**, e1001326 (2012).
16. Souza-Silva, N. G. *et al.* A Genetic Profile of Refractory Individuals with Major Depressive Disorder and Their Responsiveness to Transcranial Magnetic Stimulation. *Brain Stimul* **13**, 1091–1093 (2020).
17. Hodgson, K., Mufti, S. J., Uher, R. & McGuffin, P. Genome-wide approaches to antidepressant treatment: working towards understanding and predicting response. *Genome Med* **4**, 52 (2012).
18. Pain, O. *et al.* Antidepressant Response in Major Depressive Disorder: A Genome-wide Association Study. *medRxiv [preprint]* (2020) doi:10.1101/2020.12.11.20245035.
19. Fabbri, C., Montgomery, S., Lewis, C. M. & Serretti, A. Genetics and major depressive disorder: clinical implications for disease risk, prognosis and treatment. *Int Clin Psychopharmacol* **35**, 233–242 (2020).
20. Anderson, K. M. *et al.* Convergent molecular, cellular, and cortical neuroimaging signatures of major depressive disorder. *Proc Natl Acad Sci U S A* **117**, 25138–25149 (2020).
21. García-Gonzáleza, J. *et al.* Pharmacogenetics of antidepressant response: A polygenic approach. *Prog Neuropsychopharmacol Biol Psychiatry* **75**, 128–134 (2017).
22. Ward, J. *et al.* Polygenic risk scores for major depressive disorder and neuroticism as predictors of antidepressant response: Meta-analysis of three treatment cohorts. *PLoS One* **13**, e0203896 (2018).
23. Foo, J. C. *et al.* Evidence for increased genetic risk load for major depression in patients assigned to electroconvulsive therapy. *Am J Med Genet B Neuropsychiatr Genet* **180**, 35–45 (2019).
24. Li, Q. S., Wajs, E., Ochs-Ross, R., Singh, J. & Drevets, W. C. Genome-wide association study and polygenic risk score analysis of esketamine treatment response. *Sci Rep* **10**, 12649 (2020).
25. Amare, A. T., Schubert, K. O. & Baune, B. T. Pharmacogenomics in the treatment of mood disorders: Strategies and Opportunities for personalized psychiatry. *EPMA J* **8**, 211–227 (2017).
26. Silva, F. L. da. EEG and MEG: Relevance to Neuroscience. *Neuron* **80**, 1112–1128 (2013).

27. Zietsch, B. P. *et al.* Common and specific genetic influences on EEG power bands delta, theta, alpha, and beta. *Biol Psychol* **75**, 154–164 (2007).
28. Beijsterveldt, C. E. van, Molenaar, P. C., Geus, E. J. de & Boomsma, D. I. Heritability of Human Brain Functioning as Assessed by Electroencephalography. *Am J Hum Genet* **58**, 562–73 (1996).
29. Smit, D. J. A., Posthuma, D., Boomsma, D. I. & Geus, E. J. C. de. Heritability of background EEG across the power spectrum. *Psychophysiology* **42**, 691–697 (2005).
30. Smit, C. M., Wright, M. J., Hansell, N. K., Geffen, G. M. & Martin, N. G. Genetic variation of individual alpha frequency (IAF) and alpha power in a large adolescent twin sample. *Int J Psychophysiol* **61**, 235–243 (2006).
31. Posthuma, D. *et al.* Genetic Components of Functional Connectivity in the Brain: The Heritability of Synchronization Likelihood. *Hum Brain Mapp* **26**, 191–198 (2005).
32. Schutte, N. M. *et al.* Heritability of Resting State EEG Functional Connectivity Patterns. *Twin Res Hum Genet* **16**, 962–969 (2013).
33. Smit, D. J. A. *et al.* Endophenotypes in a Dynamically Connected Brain. *Behav Genet* **40**, 167–177 (2010).
34. Arns, M., Gordon, E. & Boutros, N. N. EEG Abnormalities Are Associated With Poorer Depressive Symptom Outcomes With Escitalopram and Venlafaxine-XR, but Not Sertraline: Results From the Multicenter Randomized iSPOT-D Study. *Clin EEG Neurosci* **48**, 33–40 (2017).
35. Arns, M. *et al.* EEG alpha asymmetry as a gender-specific predictor of outcome to acute treatment with different antidepressant medications in the randomized iSPOT-D study. *Clin Neurophysiol* **127**, 509–19 (2016).
36. Olbrich, S. & Arns, M. EEG biomarkers in major depressive disorder: Discriminative power and prediction of treatment response. *Int Rev Psychiatr* **25**, 604–618 (2013).
37. Arns, M., Cerquera, A., Gutiérrez, R. M., Hasselman, F. & Freund, J. A. Non-linear EEG analyses predict non-response to rTMS treatment in major depressive disorder. *Clin Neurophysiol* **125**, 1392–1399 (2014).
38. Erguzel, T. T. *et al.* Neural Network Based Response Prediction of rTMS in Major Depressive Disorder Using QEEG Cordance. *Psychiatry Investig* **12**, 61–65 (2014).
39. Hasanzadeh, F., Mohebbi, M. & Rostami, R. Prediction of rTMS treatment response in major depressive disorder using machine learning techniques and nonlinear features of EEG signal. *J Affect Disord* **256**, 132–142 (2019).
40. Roelofs, C. *et al.* Individual alpha frequency proximity associated with repetitive transcranial magnetic stimulation outcome: An independent replication study from the ICON-DB consortium. *Clin Neurophysiol* **S1388-2457**, 30532–0 (2020).
41. Iseger, T. A. *et al.* EEG connectivity between the subgenual anterior cingulate and prefrontal cortices in response to antidepressant medication. *Eur Neuropsychopharmacol* **27**, 301–312 (2017).

42. Dinteren, R. van *et al.* Utility of event-related potentials in predicting antidepressant treatment response: an iSPOT-D report. *Eur Neuropsychopharmacol* **25**, 1981–1990 (2015).
43. Widge, A. S. *et al.* Electroencephalographic biomarkers for treatment response prediction in major depressive illness: a meta-analysis. *Am J Psychiatry* **176**, 44–56 (2019).
44. Wu, W. *et al.* An electroencephalographic signature predicts antidepressant response in major depression. *Nat Biotechnol* **38**, 439–447 (2020).
45. Zhang, Y. *et al.* Identification of psychiatric disorder subtypes from functional connectivity patterns in resting-state electroencephalography. *Nat Biomed Eng* 1–15 (2020) doi:10.1038/s41551-020-00614-8.
46. Michel, C. M. & Pascual-Leone, A. Predicting antidepressant response by electroencephalography. *Nat Biotechnol* **38**, 417–419 (2020).
47. Gerrits, B. *et al.* Probing the "Default Network Interference Hypothesis" With EEG: An RDoC Approach Focused on Attention. *Clin EEG Neurosci* **50**, 404–412 (2019).
48. Aoki, Y. *et al.* Detection of EEG-resting state independent networks by eLORETA-ICA method. *Front Hum Neurosci* **9**, 31 (2015).
49. Krepel, N., Rush, A. J., Iseger, T. A., Sack, A. T. & Arns, M. Can psychological features predict antidepressant response to rTMS? A Discovery–Replication approach. *Psychol Med* 1–9 (2019) doi:10.1017/s0033291718004191.
50. Vinne, N. van der, Vollebregt, M. A., Putten, M. J. A. M. van & Arns, M. Frontal alpha asymmetry as a diagnostic marker in depression: Fact or fiction? A meta-analysis. *Neuroimage Clin* **16**, 79–87 (2017).
51. Saveanu, R. *et al.* The International Study to Predict Optimized Treatment in Depression (iSPOT-D): Outcomes from the acute phase of antidepressant treatment. *J Psychiatr Res* **61**, 1–12 (2015).
52. Voigt, J., Carpenter, L. & Leuchter, A. A systematic literature review of the clinical efficacy of repetitive transcranial magnetic stimulation (rTMS) in non-treatment resistant patients with major depressive disorder. *BMC Psychiatry* **19**, 13 (2019).
53. Barth, M. *et al.* Efficacy of selective serotonin reuptake inhibitors and adverse events: meta-regression and mediation analysis of placebo-controlled trials. *Br J Psychiatry* **208**, 114–119 (2016).
54. Simon, G. E. Evidence review: efficacy and effectiveness of antidepressant treatment in primary care. *Gen Hosp Psychiat* **24**, 213–224 (2002).
55. Demyttenaere, K. *et al.* Compliance With Antidepressants in a Primary Care Setting, 1: Beyond Lack of Efficacy and Adverse Events. *J Clin Psychiatry* **62**, 30–33 (2001).
56. Mullins, C. D., Shaya, F. T., Meng, F., Wang, J. & Harrison, D. Persistence, Switching, and Discontinuation Rates Among Patients Receiving Sertraline, Paroxetine, and Citalopram. *Pharmacotherapy* **25**, 660–667 (2005).
57. Goethe, J. W., Woolley, S. B., Cardoni, A. A., Woznicki, B. A. & Piez, D. A. Selective Serotonin Reuptake Inhibitor Discontinuation: Side Effects and Other Factors That Influence Medication Adherence. *J*

Clin Psychopharmacol **27**, 451–458 (2007).

58. Fonseka, T. M., MacQueen, G. M. & Kennedy, S. H. Neuroimaging biomarkers as predictors of treatment outcome in Major Depressive Disorder. *J Affect Disord* **233**, 21–35 (2018).
59. Fox, M. D., Buckner, R. L., White, M. P., Greicius, M. D. & Pascual-Leone, A. Efficacy of transcranial magnetic stimulation targets for depression is related to intrinsic functional connectivity with the subgenual cingulate. *Biol Psychiatry* **72**, 595–603 (2012).
60. Iseger, T. A., Bueren, N. E. R. van, Kenemans, J. L., Gevirtz, R. & Arns, M. A frontal-vagal network theory for Major Depressive Disorder: Implications for optimizing neuromodulation techniques. *Brain Stimul* **13**, 1–9 (2020).
61. Bedwell, S. A., Billett, E. E., Crofts, J. J. & Tinsley, C. J. The topology of connections between rat prefrontal, motor and sensory cortices. *Front Syst Neurosci* **8**, 177 (2014).
62. Liston, C. *et al.* Default mode network mechanisms of transcranial magnetic stimulation in depression. *Biol Psychiatry* **76**, 517–526 (2014).
63. Huang, C.-C., Wei, I.-H., Chou, Y.-H. & Su, T.-P. Effect of age, gender, menopausal status, and ovarian hormonal level on rTMS in treatment-resistant depression. *Psychoneuroendocrinology* **33**, 821–831 (2018).
64. Kedzior, K. K., Azorina, V. & Reitz, S. K. More female patients and fewer stimuli per session are associated with the short-term antidepressant properties of repetitive transcranial magnetic stimulation (rTMS): a meta-analysis of 54 sham-controlled studies published between 1997–2013. *Neuropsych Dis Treat* **10**, 727–756 (2014).
65. Sackeim, H. A. *et al.* Clinical outcomes in a large registry of patients with major depressive disorder treated with Transcranial Magnetic Stimulation. *J Affect Disord* **277**, 65–74 (2020).
66. Trevaskis, J. *et al.* Src homology 3-domain growth factor receptor-bound 2-like (endophilin) interacting protein 1, a novel neuronal protein that regulates energy balance. *Endocrinology* **146**, 3757–3764 (2005).
67. Bänziger, C. *et al.* Wntless, a conserved membrane protein dedicated to the secretion of Wnt proteins from signaling cells. *Cell* **125**, 509–522 (2006).
68. Petko, J., Tranchina, T., Patel, G., Levenson, R. & Justice-Bitner, S. Identifying novel members of the Wntless interactome through genetic and candidate gene approaches. *Brain Res Bull* **138**, 96–105 (2018).
69. Tatsumia, M., Groshan, K., Blakely, R. D. & Richelson, E. Pharmacological profile of antidepressants and related compounds at human monoamine transporters. *Eur J Pharmacol* **340**, 249–258 (1997).
70. Kitaichi, Y. *et al.* Sertraline increases extracellular levels not only of serotonin, but also of dopamine in the nucleus accumbens and striatum of rats. *Eur J Pharmacol* **647**, 90–96 (2010).
71. Strafella, A. P., Paus, T., Barrett, J. & Dagher, A. Repetitive Transcranial Magnetic Stimulation of the Human Prefrontal Cortex Induces Dopamine Release in the Caudate Nucleus. *J Neurosci* **21**, RC157–RC157 (2001).

72. Dunlop, B. W. & Nemeroff, C. B. The role of dopamine in the pathophysiology of depression. *Arch Gen Psychiatry* **64**, 327–337 (2007).
73. Belujon, P. & Grace, A. A. Dopamine System Dysregulation in Major Depressive Disorders. *Int J Neuropsychopharmacol* **20**, 1036–1046 (2017).
74. Geyer, M. A., Swerdlow, N. R., Mansbach, R. S. & Braff, D. L. Startle response models of sensorimotor gating and habituation deficits in schizophrenia. *Brain Res Bull* **25**, 485–498 (1990).
75. Canbeyli, R. Sensorimotor modulation of mood and depression: an integrative review. *Brain Res* **207**, 249–264 (2010).
76. Canbeyli, R. Sensorimotor modulation of mood and depression: in search of an optimal mode of stimulation. *Front Hum Neurosci* **7**, 428 (2013).
77. Donse, L., Padberg, F., Sack, A. T., Rush, A. J. & Arns, M. Simultaneous rTMS and psychotherapy in major depressive disorder: Clinical outcomes and predictors from a large naturalistic study. *Brain Stimul* **11**, 337–345 (2017).
78. Arns, M. *et al.* Frontal and rostral anterior cingulate (rACC) theta EEG in depression: Implications for treatment outcome? *Eur Neuropsychopharmacol* **25**, 1190–1200 (2015).
79. De, R., Bush, W. S. & Moore, J. H. Bioinformatics Challenges in Genome-Wide Association Studies (GWAS). in *Clinical Bioinformatics* (ed. Trent, R.) vol. 1168 63–81 (Humana Press, 2014).
80. Purcell, S. *et al.* PLINK: A Tool Set for Whole-Genome Association and Population-Based Linkage Analyses. *Am J Hum Genet* **81**, 559–575 (2007).
81. Das, S. *et al.* Next-generation genotype imputation service and methods. *Nat Genet* **48**, 1284–1287 (2016).
82. Howard, D. M. *et al.* Genome-wide meta-analysis of depression identifies 102 independent variants and highlights the importance of the prefrontal brain regions. *Nat Neurosci* **22**, 343–352 (2019).
83. Choi, S. W., Mak, T. S.-H. & O'Reilly, P. F. Tutorial: a guide to performing polygenic risk score analyses. *Nat Protoc* **15**, 2759–2772 (2020).
84. Chang, C. C. *et al.* Second-generation PLINK: rising to the challenge of larger and richer datasets. *Gigascience* **4**, 7 (2015).
85. Schür, R. R. *et al.* The effect of genetic vulnerability and military deployment on the development of post-traumatic stress disorder and depressive symptoms. *Eur Neuropsychopharmacol* **29**, 405–415 (2019).
86. McLaughlin, R. L. *et al.* Genetic correlation between amyotrophic lateral sclerosis and schizophrenia. *Nat Commun* **8**, 14774 (2017).
87. Purcell, S. M. *et al.* Common polygenic variation contributes to risk of schizophrenia and bipolar disorder. *Nature* **460**, 748–752 (2009).
88. Gratton, G., Coles, M. G. H. & Donchin, E. A new method for off-line removal of ocular artifact. *Electroencephalogr Clin Neurophysiol* **55**, 468–484 (1983).

89. Pascual-Marqui, R. D. *et al.* Assessing interactions in the brain with exact low-resolution electromagnetic tomography. *Philos Trans A Math Phys Eng Sci* **369**, 3768–3784 (2011).
90. Calhoun, V. D., Liu, J. & Adali, T. A review of group ICA for fMRI data and ICA for joint inference of imaging, genetic, and ERP data. *Neuroimage* **45**, S163-172 (2009).
91. Pascual-Marqui, R. D. & Biscay-Lirio, R. J. Interaction patterns of brain activity across space, time and frequency. Part I: methods. (2011).
92. Wackermann, J. Beyond mapping: estimating complexity of multichannel EEG recordings. *Acta Neurobiol Exp (Wars)* **56**, 197–208 (1996).
93. Glischinski, M. von, Brachel, R. von & Hirschfeld, G. How depressed is “depressed”? A systematic review and diagnostic meta-analysis of optimal cut points for the Beck Depression Inventory revised (BDI-II). *Qual Life Res* **28**, 1111–1118 (2019).
94. Rush, A. J. *et al.* The 16-Item Quick Inventory of Depressive Symptomatology (QIDS), clinician rating (QIDS-C), and self-report (QIDS-SR): a psychometric evaluation in patients with chronic major depression. *Biol Psychiatry* **54**, 573–583 (2003).
95. Johnson, V. E. Revised standards for statistical evidence. *Proc Natl Acad Sci U S A* **110**, 19313–19317 (2013).

Table

Table 1 *Baseline characteristics*

Baseline characteristics	*Dataset 1*	*Dataset 2: rTMS*	*Dataset 3: medication*
Total number participants, N included for statistical analysis	1,195 1,123	196 186	1,008 535
Ratio male/female participants	617/506	93/93	245/290
Mean age (SD), years	40.3 (13.2)	43.3 (12.9)	38.5 (12.6)
Self-reporting questionnaire; mean baseline score (SD)	BDI-II; 31.1 (12.1)	BDI-II; 30.8 (9.8)	QIDS; 14.5 (3.7)
Remission and response rate (%)	N/A	55.4; 66.1	35.3; 48.8

Abbreviations: BDI-II=Beck Inventory Index, second version; QIDS=Quick Inventory of Depressive Symptomatology.
N/A as this was a non-intervention study no treatment effects were assessed.

Figures

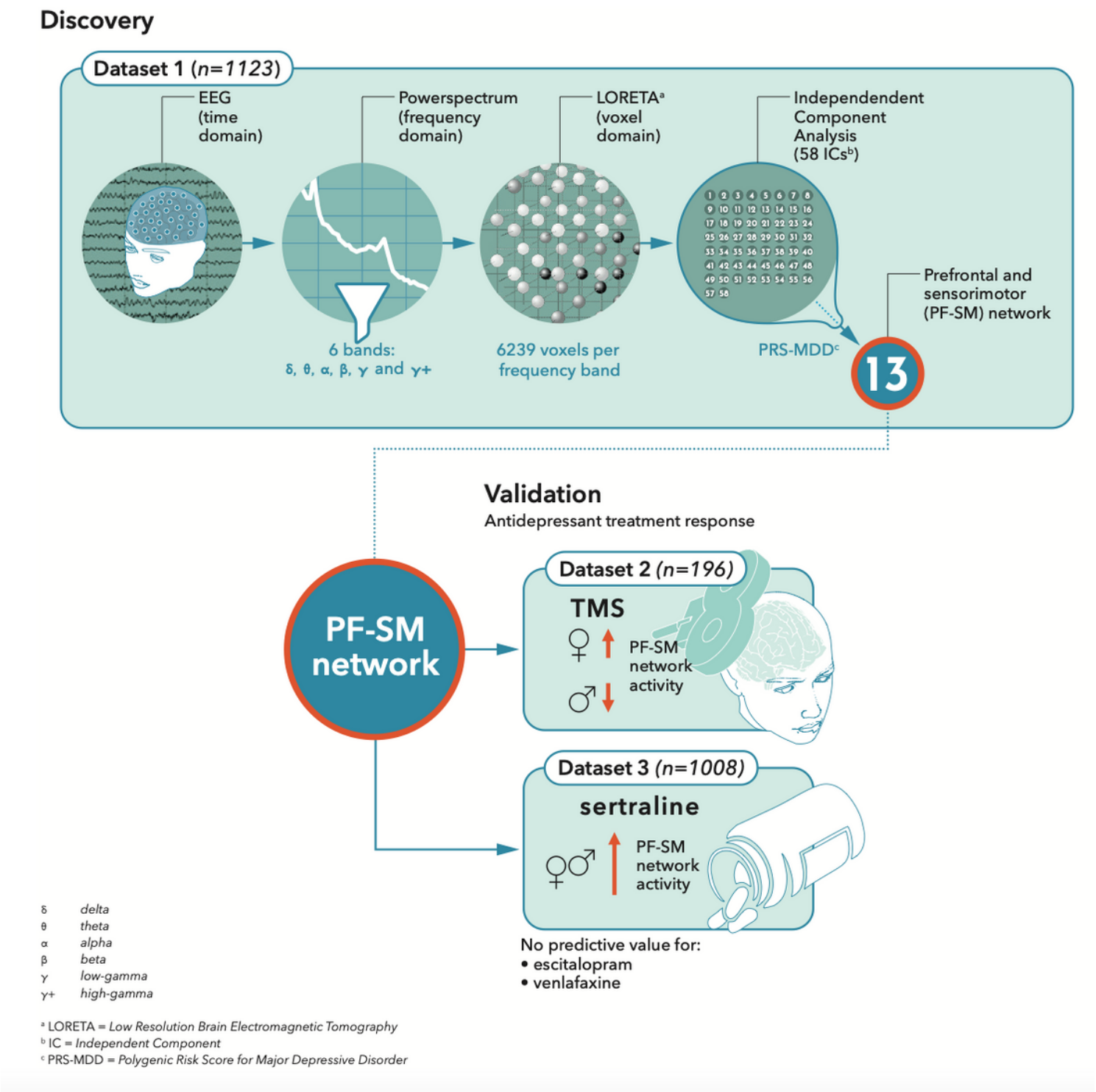

Figure 1

Chart depicting the study set-up and analysis pipeline. The discovery analysis (dataset 1) using the fICA-LORETA method is shown left. Data for the functional independent component analysis (fICA) consisted of 6 a priori defined frequency bands and 6239 voxels (6x6239) per subject. This resulted in 58 independent cross-frequency spectral-spatial components. EEG component 13 (i.e. PF-SM network) was robustly associated with PRS-MDD. This component was used for validation in two independent datasets: MDD patients treated with rTMS and concurrent psychotherapy (dataset 2) and

pharmacotherapy (dataset 3), which is shown on the right. PF-SM network activity was differentially associated with rTMS response while similarly associated with sertraline response in men and women. Network activity was not associated with escitalopram or venlafaxine response.

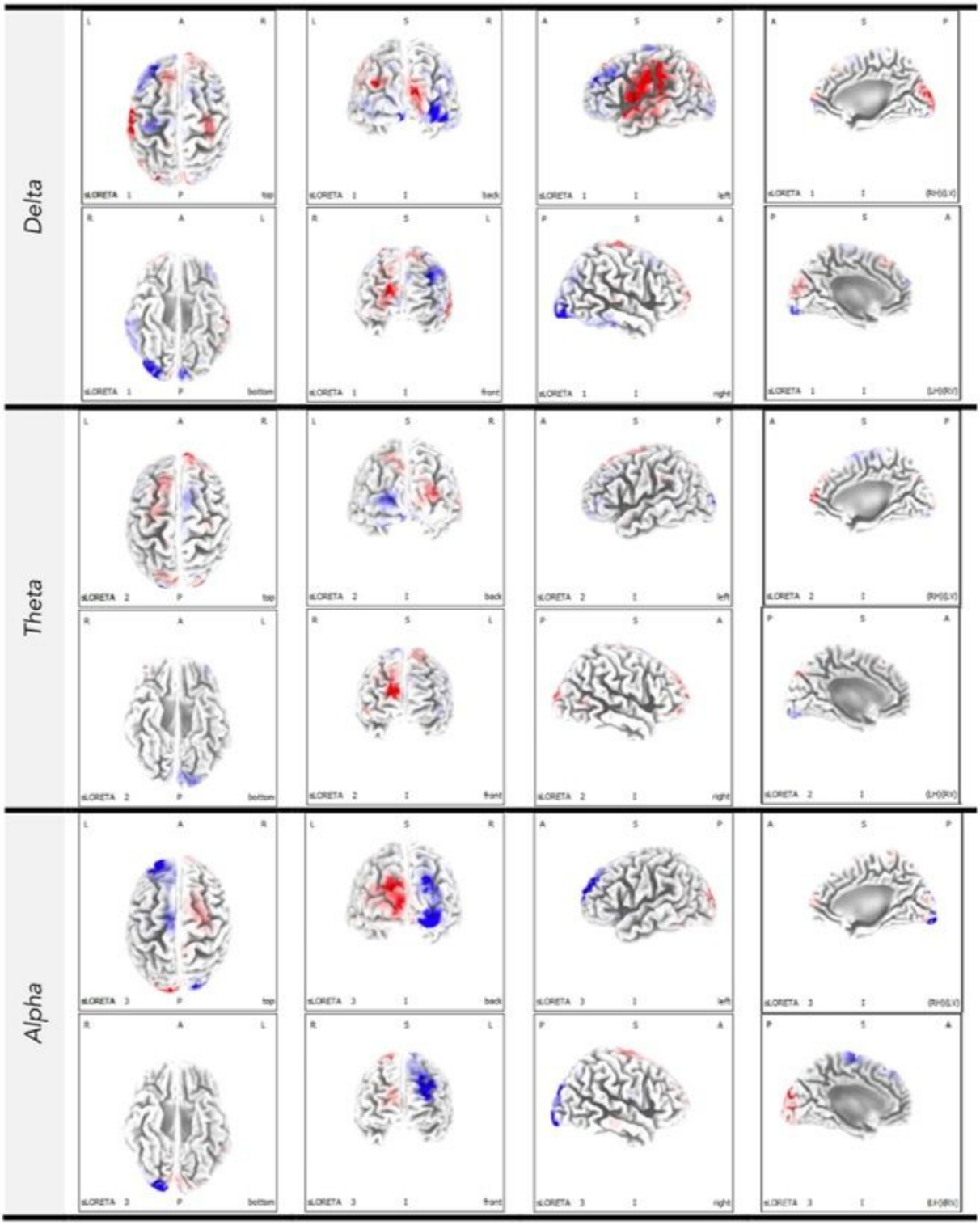

Figure 2

Functional network of the component obtained with LORETA-ICA. Scaled map of the EEG functional network obtained in this study using LORETA-ICA (independent component 13). The colors represent

correlated and inversely correlated EEG power changes of brain regions (when neural activity in red colored regions inceases, activity in blue colored regions decreases, and vice versa). The component covers activity within the delta, theta and alpha frequency bands in different parts of the brain. Frontally (Brodmann area [BA] 6 and 8 to 10), left-sided alpha power is inversely correlated with right-sided delta and theta power. Occipitally (BA 17 to 19), there is a notable right-left asymmetric neural activation (i.e. negative correlation), inversely for alpha and theta power, whereas there is a diffuse activation and deactivation of delta power. Most evident is delta activation seen at a large area surrounding the left lateral sulcus including parts of the parietal (somatosensory cortex, BA 1 to 3; supramarginal gyrus, BA 40), temporal (Wernicke's area, BA 22), and frontal (motor cortex, BA 4 and 6; Broca's area, BA 44) lobe. Given the participating brain regions, we termed this network the prefrontal-sensorimotor (PF-SM) network.

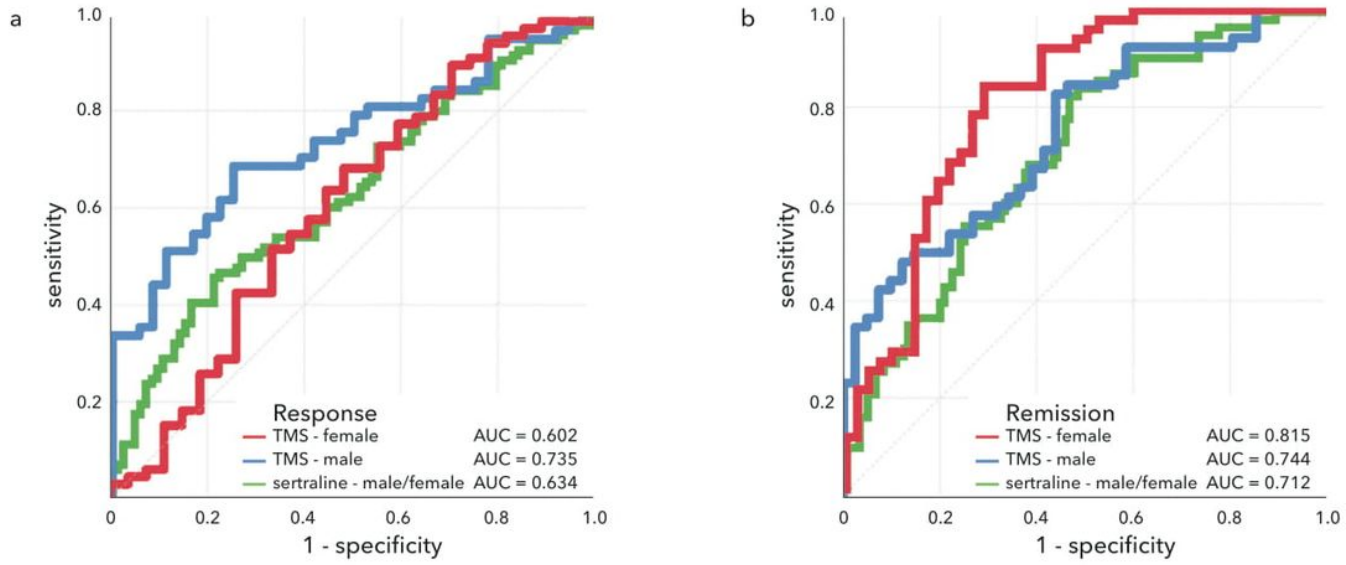

Figure 3

ROC curves of the improved treatment prediction models. ROC (receiver operating characteristic) curves for the prediction of response (A) and remission (B) by the prefrontal-sensorimotor (PF-SM) network loading and age, and baseline symptom severity score in case of remission. Red and blue lines represent outcome after rTMS treatment in women and men, respectively (dataset 2). Green lines represent outcome after sertraline treatment in women and men (dataset 3). The area under the curve (AUC) for each model is displayed in the figure.

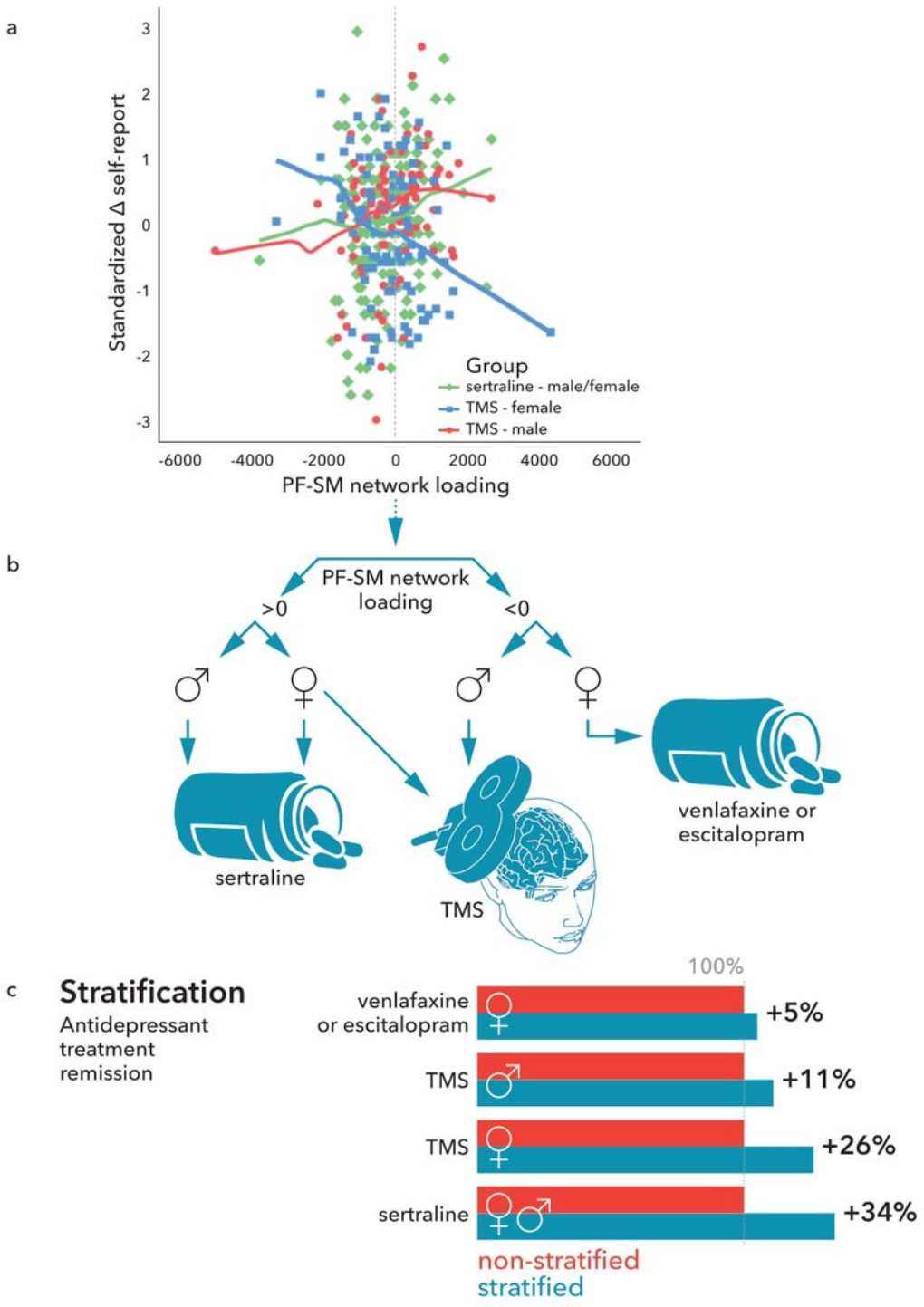

Figure 4

Stratification based on PF-SM network loading. The scatterplot (A) displays the change on the self-report questionnaires (standardized ΔBDI-II for the rTMS sample and ΔQIDS for the sertraline sample; positive values indicate improvement and negative values worsening of symptoms) and the individual loading on the prefrontal-sensorimotor (PF-SM) network. The colored lines represent the LOESS (locally estimated scatterplot smoothing; 75% points to fit) within the specified group. The grey vertical dotted line represents a clinical useful cut-off to guide treatment, which is determined to be zero. The simulation (B)

was based on the findings under A, and allocated patients to different antidepressant treatments depending their network PF-SM loading (>0 or <0) and sex. The bar chart (C) represents the improvement of treatment remission after stratification (blue bars) relative to normalized remission rates without stratification (red bars) if patients were stratified according to the simulation under B.

Supplementary Files

This is a list of supplementary files associated with this preprint. Click to download.

- GeneticsinformedEEGbiomarkersupplementary.docx